

Melanoma mouse model implicates metabotropic glutamate signaling in melanocytic neoplasia

Pamela M. Pollock^{1*}, Karine Cohen-Solal^{2*}, Raman Sood^{1*}, Jin Namkoong², Jeffrey J. Martino², Aruna Koganti², Hua Zhu², Christiane Robbins¹, Izabela Makalowska³, Seung-Shick Shin², Yari Marin², Kathleen G. Roberts⁴, Laura M. Yudt¹, Amy Chen⁵, Jun Cheng⁵, Arturo Incao⁵, Heather W. Pinkett¹, Christopher L. Graham¹, Karen Dunn⁵, Steven M. Crespo-Carbone², Kerine R. Mackason², Kevin B. Ryan², Daniel Sinsimer², James Goydos^{6,7}, Kenneth R. Reuhl⁴, Michael Eckhaus⁸, Paul S. Meltzer¹, William J. Pavan⁵, Jeffrey M. Trent¹ & Suzie Chen^{2,7}

*These authors contributed equally to this work.

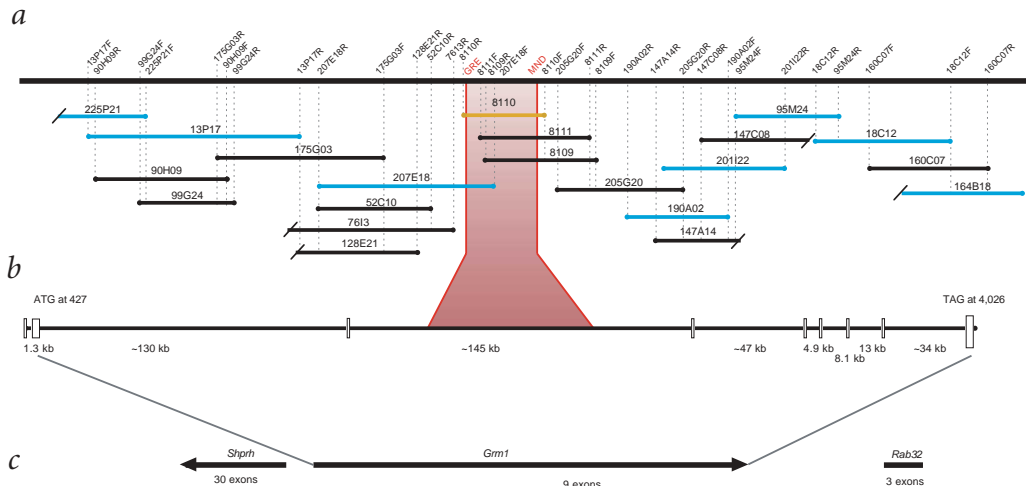
Published online 21 April 2003; doi:10.1038/ng1148

To gain insight into melanoma pathogenesis, we characterized an insertional mouse mutant, TG3, that is predisposed to develop multiple melanomas^{1,2}. Physical mapping identified multiple tandem insertions of the transgene into intron 3 of *Grm1* (encoding metabotropic glutamate receptor 1) with concomitant deletion of 70 kb of intronic sequence. To assess whether this insertional mutagenesis event results in alteration of transcriptional regulation, we analyzed *Grm1* and two flanking genes for aberrant expression in melanomas from TG3 mice. We observed aberrant expression of only *Grm1*. Although we did not detect its expression in normal mouse melanocytes, *Grm1* was ectopically expressed in the melanomas from TG3

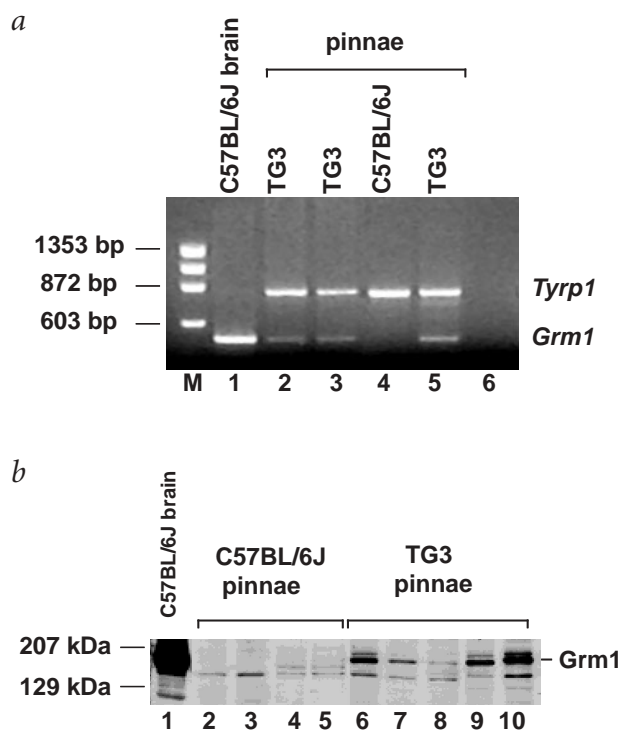
mice. To confirm the involvement of *Grm1* in melanocytic neoplasia, we created an additional transgenic line with *Grm1* expression driven by the dopachrome tautomerase promoter. Similar to the original TG3, the Tg(*Grm1*)EPv line was susceptible to melanoma. In contrast to human melanoma, these transgenic mice had a generalized hyperproliferation of melanocytes with limited transformation to fully malignant metastasis. We detected expression of GRM1 in a number of human melanoma biopsies and cell lines but not in benign nevi and melanocytes. This study provides compelling evidence for the importance of metabotropic glutamate signaling in melanocytic neoplasia.

Fig. 1 Physical and transcript map of the genomic region of roughly 1 Mb flanking the TG3 transgene integration site on mouse chromosome 10. **a**, The solid black line at the top represents a portion of mouse chromosome 10. The unique sequences flanking the transgene integration site, MND and GRE (red typeface) were identified after screening a genomic library from a TG3 mouse with the clone B transgene sequence. These sequences were then used to identify several BAC clones to initiate the contig. BAC ends were sequenced to design new STS markers (shown at top) for further walking.

BAC end sequences containing repeats are indicated by a diagonal line. Shotgun sample sequencing of several BACs (solid blue lines) was done. BAC8110 (solid orange line) containing the deleted region was completely sequenced. **b**, Genomic structure of *Grm1*. Open boxes represent exons with the ATG occurring in exon 2 and the stop codon in exon 9. Precise intron size is indicated where available from mouse genomic sequence analysis; estimated intron size based on the orthologous human sequence is given in other cases. The extent of the deletion in the TG3 insertional mouse mutant is indicated with red shading. **c**, Transcript map indicating *Grm1* (ref. 18), *Rab32* (K.C.-S., R.S., Y.M., S.M.C.-C., D.S., J.J.M., C.R., I.M., J.M.T. and S.C., manuscript submitted) and a new gene, *Shprh*, with similarity to helicases¹⁹. Arrows indicate the orientation of transcription (5' to 3') if known.



¹Cancer Genetics Branch, National Human Genome Research Institute, National Institutes of Health, Bethesda, Maryland 20892, USA. ²Susan Lehman Cullman Laboratory for Cancer Research, Department of Chemical Biology, Ernest Mario School of Pharmacy, Rutgers, The State University of New Jersey, Piscataway, New Jersey 08854, USA. ³Genome Technology Branch, National Human Genome Research Institute, National Institutes of Health, Bethesda, Maryland 20892, USA. ⁴Department of Pharmacology and Toxicology, Ernest Mario School of Pharmacy, Rutgers, The State University of New Jersey, Piscataway, New Jersey 08854, USA. ⁵Genetic Disease Research Branch, National Human Genome Research Institute, National Institutes of Health, Bethesda, Maryland 20892, USA. ⁶Department of Surgery, UMDNJ-Robert Wood Johnson Medical School, 675 Hoes Lane, Piscataway, New Jersey 08854, USA. ⁷The Cancer Institute of New Jersey, 195 Little Albany Street, New Brunswick, New Jersey 08903, USA. ⁸Veterinary Resources Program, Office of Research Services, National Institutes of Health, Bethesda, Maryland, 20892, USA. Correspondence should be addressed to S.C. (e-mail: suziec@rci.rutgers.edu).



Melanoma incidence and mortality rates in European populations are increasing worldwide. Approximately 10% of melanomas occur in individuals with familial predisposition, but loci associated with susceptibility to multiple melanomas have yet to be identified. Spontaneous and induced mouse mutants are tools for uncovering new genes and pathways implicated in a particular disease. An insertional mouse mutant, TG3, was generated by pronuclear injection with a 2-kb genomic fragment, clone B³. This previously described TG3 line is predisposed to develop multiple melanomas primarily affecting the pinnae of the ear, perianal region, eyelid, snout, trunk and legs^{1,2}. Metastases to distant organs were detected in some cases^{1,2}. Melanoma susceptibility was found to be linked with the presence of the transgene.

Fig. 2 Ectopic expression of *Grm1* in melanomas from TG3 mice. The pinnae are one of the sites of primary melanoma formation in TG3 mice, and these tumors are comprised mostly of melanocytic tumor cells (>90%) with very few normal melanocytes^{2,20}. **a**, Duplex RT-PCR showing expression of *Grm1* in pinnae with tumors from TG3 mice (lanes 2, 3 and 5) but not pinnae from C57BL/6J mice (lane 4) when equivalent numbers of melanocytes were analyzed, as evidenced by similar *Tyrp1* expression levels. M, PhiX174DNA/*Hae*III marker (Promega); lane 1, brain is the positive control for *Grm1* expression; lane 6, water. **b**, Western-blot analysis using antibody against *Grm1* (Upstate Biotechnology) showing absence of *Grm1* expression in pinnae from wild-type mice (lanes 2–5) and high expression in tumor pinnae from TG3 mice (lanes 6–10). Expression of *Grm1* in brain is a positive control (lane 1). 20 µg of total protein was loaded for each sample.

We localized the transgene insertion site to mouse chromosome 10 in a region orthologous to human chromosome band 6q23–24. Physical mapping identified multiple tandem insertions of the transgene into intron 3 of *Grm1* (also called *Gprc1a* and *mGluR1*) and this integration event resulted in the deletion of 70 kb of intronic sequence. The physical map we created spans a genomic region of roughly 1 Mb flanking the integration site. We determined the full-length sequence of *Grm1* and cloned cDNAs of two flanking genes, *Rab32* and *Shprh* (Fig. 1). We reasoned that the melanoma phenotype observed in the TG3 line was due to aberrant gene expression of either *Grm1* or a flanking gene. This could be a result of the presence of the transgene itself, the deletion of an essential regulatory element in the intronic sequence or a complex interaction between the transgene and regulatory elements in or near the deleted region.

We initially evaluated the tissue-specific expression of *Grm1*, *Rab32* and *Shprh* by northern-blot analysis. In normal tissues, we detected expression of *Grm1* in the brain, heart and kidney but not in placenta, lung, liver, skeletal muscle or pancreas. In contrast, both *Rab32* and *Shprh* were expressed, albeit at varying levels, in all tissues examined (data not shown). We also investigated these three genes for aberrant expression in melanomas removed from TG3 mice by RT-PCR and western blotting. Notably, we detected expression of *Grm1* by both RT-PCR and western blotting in pinnae tumors but not in the mouse melanocyte cell line melan-a (data not shown) or in normal pinnae (Fig. 2). To control for differing melanocyte number in normal and tumor pinnae, we carried out duplex RT-PCR with the melanocyte-specific marker *Tyrp1*. When the level of *Tyrp1* expression was comparable in normal and tumor pinnae, we detected *Grm1* expression

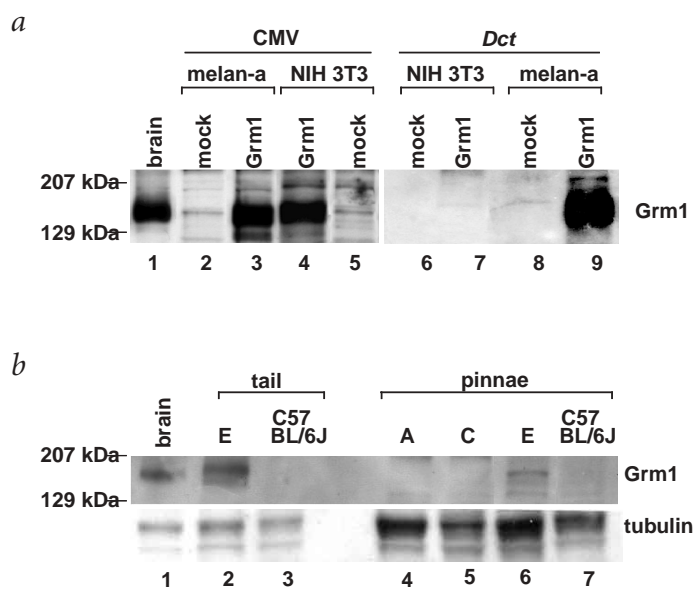


Fig. 3 Expression of *Grm1* in transiently transfected cells and tumors. **a**, *Dct* expression construct directs expression of *Grm1* in melan-a cells but not NIH3T3 cells after transient transfection. Protein extracts isolated 48 h after transfection were probed with antibody against *Grm1*. Lane 1, C57BL/6J brain (positive control); lanes 2–5, transient transfection of CMV vector (mock) or CMV-*Grm1* into melan-a cells (lanes 2 and 3, respectively) or NIH3T3 cells (lanes 5 and 4, respectively); lanes 6–9, transient transfection of *Dct*-vector (mock) or *Dct*-*Grm1* into NIH3T3 cells (lanes 6 and 7, respectively) or melan-a cells (lanes 8 and 9, respectively). Note CMV directed expression in both NIH3T3 and melan-a cells, whereas *Dct* targeted expression of *Grm1* in melan-a cells only (lane 9 versus lane 7). A total of 25 µg of protein extract from each sample was loaded in each lane. **b**, Absence of *Grm1* expression in transgenic lines lacking melanoma phenotype. Western-blot analysis using antibody against *Grm1*. Lane 1 shows results from C57BL/6J brain (positive control, 10 µg). Expression of *Grm1* was evident in a tail tumor taken from an E mouse (lane 2, 15 µg) but not a normal tail from a C57BL/6J mouse (lane 3, 15 µg). Expression of *Grm1* was observed in pinnae from an 8-wk-old E mouse (lane 6) but not pinnae from A (lane 4) or C (lane 5) transgenic lines without melanoma susceptibility. Expression was also not seen in pinnae from a similarly aged C57BL/6J mouse (lane 7). For lanes 4–7, 30 µg of protein extract was loaded in each lane. Membranes were blotted with antibody against tubulin as a loading control.

only in tumor pinnae and brain (positive control; Fig. 2a). Western blotting confirmed the ectopic expression of *Grm1* in melanoma tumors from the TG3 line and its absence in normal pinnae from C57BL/6J mice (Fig. 2b).

To show that overexpression of *Grm1* in melanocytes leads to melanocytic hyperplasia and melanoma, we created a new transgenic line in which expression of *Grm1* is targeted to the melanocytes by the dopachrome tautomerase (*Dct*) promoter⁴. This promoter sequence has previously been used to drive expression of *lacZ* specifically in melanoblasts and melanocytes⁵. After transient transfection of this *Dct-Grm1* construct into both NIH3T3 and melan-a cells, we observed expression of *Grm1* exclusively in the melanocyte cell line. In contrast, a CMV-driven construct permitted the expression of *Grm1* in both NIH3T3 and melan-a cells (Fig. 3a).

After pronuclear injection of the *Dct-Grm1* transgene, we obtained three transmitting founders from 53 live offspring. One founder, Tg(*Grm1*)EPv (E), developed pigmented lesions on the pinnae and tail at 5–6 months of age, which progressed into raised lesions by 6–7 months. Tumor burden required removal of the tail from this mouse at 14 months, and the mouse was killed at 20 months of age. To assess transgene expression, we carried out whole-mount *in situ* hybridization on 12.5-d-old embryos from all three founder lines (A, C and E). Only transgenic embryos derived from the E line had strong expression of *Grm1* in a ubiquitous ectodermal distribution (data not shown). Therefore, it is possible that expression of *Grm1* may influence the growth of melanocytes through the release of growth factors or changes in cell adhesion by adjacent keratinocytes. To confirm that the absence of tumors in the other two lines, Tg(*Grm1*)APv (A) and Tg(*Grm1*)CPv (C), was due to lack of *Grm1* expression, we carried out western-blot analysis on pinnae from 6–8-week-old mice from all three lines. We observed expression of *Grm1* only in pinnae removed from mice derived from the E line (Fig. 3b).

All 107 transgenic offspring derived from the E line presented initially with flat hyperpigmented lesions that subsequently developed into raised overt melanomas. These lesions always affected the pinnae and tail, albeit with differing severity (Fig. 4). Over the five generations of mice we have so far monitored, tumor onset has had 100% penetrance. We have also observed flat pigmented lesions on the limbs and around the snout and, occasionally, raised tumors on the eyelid. Detailed histopathological analysis of mice from the E line shows hyperproliferation of the dermal melanocytes in the pinnae

and tail (Fig. 4). The submandibular and inguinal lymph nodes, but not distant lymph nodes, were pigmented and enlarged. We confirmed the presence of melanoma cells in the submandibular and inguinal lymph nodes by verifying expression of *Tyrp1* (Fig. 5). In contrast to TG3, we observed no gross pigmented lesions in distant organs of E mice after morphologic evaluation and no melanoma cells in a variety of distant organs including the lung, liver, kidney and spleen after histopathological analysis, even in aged mice killed because of primary tumor burden.

The predisposition towards tumor formation on the hairless skin areas rather than the trunk probably reflects the retention of dermal melanocytes in these areas compared with the postnatal reduction of dermal melanocytes in haired skin⁶. In contrast to the original TG3 insertional mutant line, the E line showed a predisposition towards tumors affecting the tail, an absence of tumors affecting the perianal region and harderian gland and an absence of metastases to distant organs. The phenotypic differences between these lines could be due to differences in the regulation of *Grm1* expression between these two lines or to the presence of the clone B transgene in TG3 mice influencing the expression of other genes. The otherwise similar clinical and histopathological phenotype is promising evidence that the susceptibility to melanoma of the original insertional mutant was due to the dysregulation of *Grm1* expression.

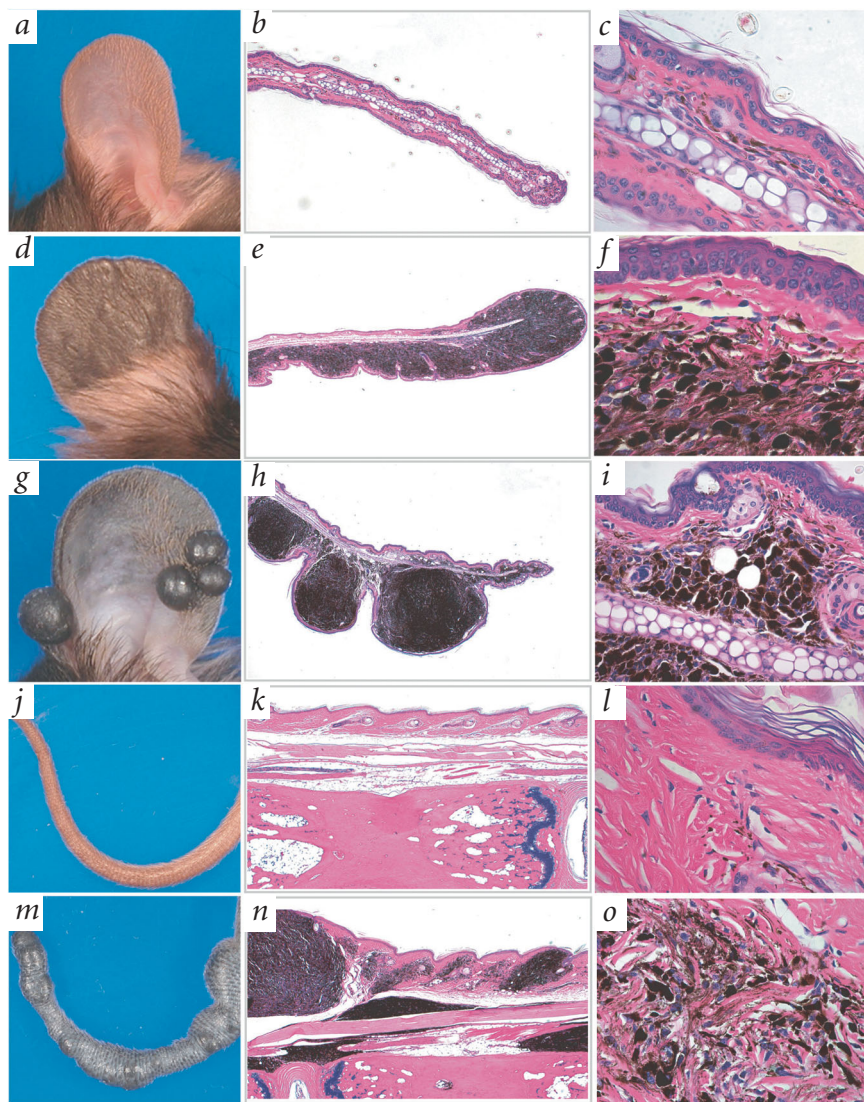


Fig. 4 Melanomas observed in E line. Compared to normal pinnae (a–c) and tail (j–l), melanomas presented as either raised nodules or a generalized thickening of the pinnae (d–f) or tail (m–o). The lesions initially presented as regions of hyperpigmentation. The melanomas present on the tail appear locally invasive, with melanoma cells often observed in the underlying muscle and ligaments (n).

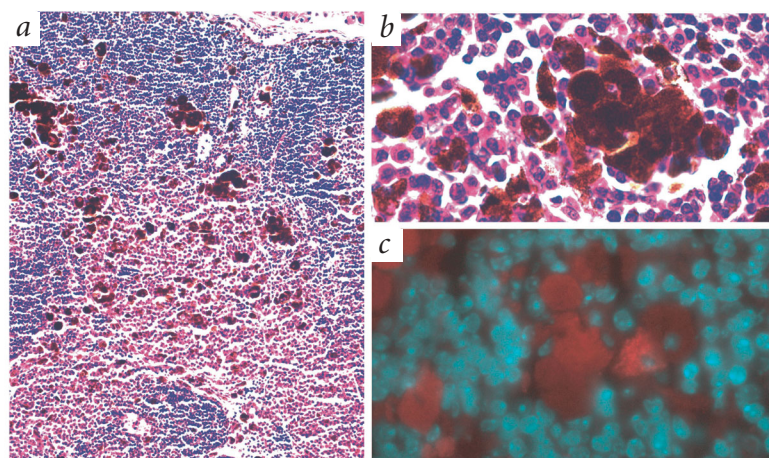


Fig. 5 Metastatic melanoma cells in lymph nodes of the 20-month-old E founder. Section of lymph node stained with hematoxylin and eosin showing extent of melanoma cell infiltration (original magnification $\times 100$ (a) and $\times 630$ (b,c). Section was stained with an antibody directed against Tyrp1 and expression detected by staining with a Cy5 conjugated secondary (red stain) and counter-stained with DAPI (blue staining). Expression of Tyrp1 was confined to the pigmented melanoma cells in the lymph node.

Glutamate is the predominant excitatory neurotransmitter in the mammalian central nervous system, and it can signal through a variety of glutamate receptors. Although once thought to be restricted to the central nervous system, glutamate signaling has been shown in a variety of non-neuronal tissues, including bone and skin⁷. There are two main categories of glutamate receptors. The ionotropic receptors are glutamate-gated, cation-specific ion channels, whereas the metabotropic receptors are coupled to intracellular signal-transduction pathways through G proteins. Metabotropic glutamate receptors are members of the large family of seven-transmembrane-domain G protein-coupled receptors. Both Grm1 and Grm5 (also called Gprc1e and mGluR5) are group I metabotropic glutamate receptors coupling primarily to phosphoinositide hydrolysis. Grm1 has also been shown to couple to multiple intracellular signaling cascades including adenylate cyclase activation⁸. Mice carrying null mutations in *Grm1* have severe deficits in motor coordination and spatial learning^{9–11}, but no melanocytic defect has been described. Metabotropic glutamate receptors have not previously been implicated in tumorigenesis; however, a variety of G protein-coupled receptors and G proteins, including those that signal through phosphoinositide hydrolysis and cAMP accumulation, have been implicated in tumorigenesis through either mutational activation or overexpression^{12,13}. In addition, glutamate has recently been linked to tumor growth in both neuronal and non-neuronal cancers^{14,15}. Most notably, glutamate has been shown to stimulate proliferation of lung carcinoma cells in serum-deprived media, and antagonists to the ionotropic

glutamate receptors, AMPA and NMDA receptors, have been shown to inhibit proliferation and increase cell death in a calcium-dependent manner in a variety of non-neuronal cancers¹⁵. Furthermore, agonist stimulation of Grm5 in subconfluent melanocyte cultures has been shown to result in melanocytic proliferation¹⁶. To extend these studies to human melanomas, we examined expression of *GRM1* in human samples. Duplex RT-PCR analysis indicated that *GRM1* was not expressed in two benign nevi but was expressed in 7 of 19 melanoma samples (Fig. 6a). Western-blot analysis likewise showed that *GRM1* was expressed in 12 of 18 melanoma cell lines but not in normal human melanocytes (Fig. 6b), warranting a more detailed investigation into the importance of *GRM1* and its downstream signaling cascade(s) to human melanoma pathogenesis. As this is the first study implicating metabotropic glutamate receptors in tumorigenesis, it also promises many additional avenues of research. These include the normal role of glutamate signaling in non-neuronal tissues, the importance of metabotropic glutamate receptors in tumorigenesis, both in neuronal and non-neuronal tissues, and the downstream signaling cascade(s) through which this receptor may exert a tumorigenic effect in these different tissues. Finally, the implication of a new signaling pathway in tumorigenesis offers an opportunity to explore additional therapeutic targets for this clinically intractable disease.

Methods

Western blotting. Using a Polytron (Brinkmann Instruments), we lysed pinnae, brain and tail tissues at 4 °C in lysis buffer (50 mM Tris-HCl, 150 mM NaCl, 1 mM EDTA, 1% Nonidet-P40, 5% glycerol and 1 mM dithiothreitol, pH 7.4) in the presence of protease inhibitors (Complete protease inhibitor cocktail tablets, Roche Applied Science). We lysed cells in the same buffer. We determined the protein concentration of each sample with Bio-Rad DC protein Assay (Bio-Rad). We loaded the amount of protein from total lysates indicated in figure legends into each lane of a 7.5% polyacrylamide gel along

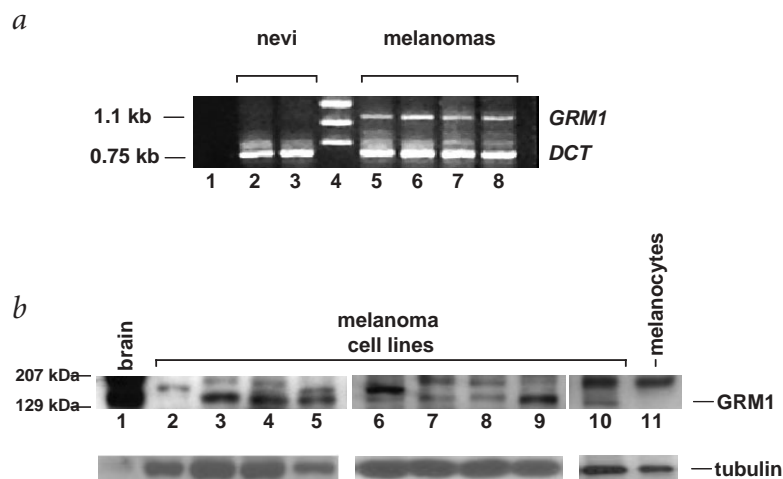


Fig. 6 Expression of *GRM1* is detectable in human melanoma samples but not in melanocytes. **a**, A total of 19 melanoma biopsy samples were examined and 7 of 19 showed detectable expression of *GRM1*. A representative duplex RT-PCR showing expression of *GRM1* in biopsies from melanomas (lanes 5–8) but not nevi (lanes 2 and 3) when equivalent numbers of melanocytes were analyzed as evidenced by similar *DCT* expression levels. lane 1, water; lanes 2 and 3, benign nevi; lane 4, PhiX174DNA/*HaellI* marker (Promega); lanes 5 and 8, nodal metastases; lane 6, primary tumor; lane 7, in-transit metastases. **b**, A total of 18 human melanoma cell lines were examined in western immunoblots and 12 of 18 showed detectable *GRM1* expression. A representative western blot showing *GRM1* expression in melanoma cell lines but not normal human melanocytes. lane 1, brain positive control; lanes 2–10, A2058, H1294, n15006, n92-047, Bowes, UACC2837, UACC1273, UACC1097 and UACC2837 cell lines, respectively; lane 11, melanocytes. 5 μ g of brain extract was loaded, otherwise 25 μ g of all other samples was loaded. Expression of *GRM1* was present in all but the A2058 cell line.

with prestained molecular weight markers (Bio-Rad). After transfer of proteins onto nitrocellulose membranes (Osmonics), we probed the membranes with a rabbit polyclonal antibody against Grm1 at 2 $\mu\text{g ml}^{-1}$ (Upstate Biotechnology) and, for the normalization experiments, also with a mouse monoclonal antibody against tubulin at 2 $\mu\text{g ml}^{-1}$ (Santa Cruz Biotechnology). We visualized bands with the Amersham ECL system. In addition, we raised antibodies to peptides derived from Rab32 and Shprh and affinity-purified them. Peptide sequences are available on request.

RT-PCR. For RNA analysis, cDNA synthesis and PCR, we purified total RNA from tissue samples with TRI REAGENT (Molecular Research Center), generated oligo-dT-primed, first-strand cDNA from the total RNA with SuperScript-II RNase H⁻ Reverse Transcriptase (Invitrogen) and completed PCR using the Taq PCR Master Mix Kit (Qiagen), according to the manufacturers' protocols. Guided by pilot reactions to obtain relatively equivalent levels of RT-PCR product from *Tyrp1* or *Dct* transcripts (using *Tyrp1* or *Dct* primers, respectively), we standardized the amount of melanocyte cDNA input into the final duplex PCR reactions carried out with primers from both *Grm1* and either *Tyrp1* or *Dct*. Primer sequences are available on request.

Transgenic construction. The construct used for microinjection contained a 3,265-bp *MspA11-StuI* fragment of the *Dct* promoter⁴ from -3181 to +445 adjacent to the *Grm1* coding sequence followed by the human growth hormone polyA¹⁷ cloned into pBSK(+). The *Grm1* sequence included 241 bp of *Grm1* intron 1 sequence and transcribed sequences corresponding to -105 to +4164. After double cesium chloride plasmid purification and excision from the plasmid by *NotI*, we gel-purified and injected the insert into the pronuclei of C57BL/6J mice.

For *Dct-Grm1* genotyping, we extracted DNA from tail biopsies using standard techniques and then analyzed the samples by a duplex PCR procedure using both *Grm1* primers and *Rapsn* control primers. Primer sequences are available on request. We obtained subsequent offspring from each of the three positive founder lines.

Immunofluorescence. We carried out immunofluorescent staining on 5 μm -thick paraffin-embedded sections of mouse lymph node. After removing the paraffin, hydrating and steaming the sections in Antigen Unmasking Solution (Vector) for 30 min, we blocked them with 5% goat serum in phosphate-buffered saline and then incubated them with the rabbit polyclonal antiserum against Tyrp1 α -PEP-1 (dilution 1:1,000) overnight at 4°C. We then incubated the sections with Cy5-conjugated goat antibody against rabbit IgG (1:1,000; Jackson ImmunoResearch) for 1 h at room temperature and finally collected images using a Zeiss Axio-phot microscope equipped with a 12-bit CCD camera.

Protocol approvals. All animal protocols were approved by the Animal Care and Use Committee of the National Human Genome Research Institute and the Animal Care and Facilities Committee of Rutgers, The State University of New Jersey, Office of Research and Sponsored Programs. We obtained human RNA and protein samples through the Tissue Retrieval Service at the Cancer Institute of New Jersey. The Institutional Review Board of the Cancer Institute of New Jersey directs the collection of human tissues in a manner to ensure patient confidentiality and informed consent, and with the Institutional Review Board of Rutgers, The State University of New Jersey, Office of Research and Sponsored Programs, approved the use of the aforementioned human samples for research purposes.

GenBank accession numbers. *Grm1*, AF320126; *Rab32*, AY135650; *Shprh*, AY162264; BAC8110, AY158230.

Acknowledgments

We thank I. Jackson and G. Merlino for the *Dct* expression construct; V. Hearing for the *Tyrp1* antibody; L. White for human melanocytes; J. Welch, M. Galdzicki and E. Eddings for technical help; and A. Weeraratna, K. Sweder, L. Wise, R. Zhou and members of W.J.P.'s laboratory for helpful discussions. This work was supported by a Collaborative Research Award from the Cancer Institute of New Jersey (S.C. and J.G.), The Ohl Cancer Foundation (S.C.), New Jersey Commission on Cancer Research (S.C.), National Cancer Institute (S.C.) and National Institute of Environmental Health Sciences (S.C. and K.R.R.). P.M.P. was supported by an Australian National Health and Medical Research Council CJ Martin postdoctoral fellowship. K.C.-S. was supported by a fellowship from La Fondation Pour la Recherche Médicale.

Competing interests statement

The authors declare that they have no competing financial interests.

Received 16 October 2002; accepted 28 March 2003.

- Chen, S., Zhu, H., Wetzel, W.J. & Philbert, M.A. Spontaneous melanocytosis in transgenic mice. *J. Invest. Dermatol.* **106**, 1145–1150 (1996).
- Zhu, H. et al. Development of heritable melanoma in transgenic mice. *J. Invest. Dermatol.* **110**, 247–252 (1998).
- Colon-Teicher, L. et al. Genomic sequences capable of committing mouse and rat fibroblasts to adipogenesis. *Nucleic Acids Res.* **21**, 2223–2228 (1993).
- Budd, P.S. & Jackson, I.J. Structure of the mouse tyrosinase-related protein-2/dopachrome tautomerase (*Tyrp2/Dct*) gene and sequence of two novel slaty alleles. *Genomics* **29**, 35–43 (1995).
- Mackenzie, M.A., Jordan, S.A., Budd, P.S. & Jackson, I.J. Activation of the receptor tyrosine kinase Kit is required for the proliferation of melanoblasts in the mouse embryo. *Dev. Biol.* **192**, 99–107 (1997).
- Reedy, M.V., Parichy, D.M., Erickson, C.A., Mason, K.A. & Frost-Mason, S.K. Regulation of Melanoblast Migration and Differentiation. in *The Pigmentary System: Physiology and Pathophysiology* (eds Nordlund, J.J., Boissy, R.E., Hearing, V.J., King, R.A. & Ortonne, J.P.) (Oxford University Press, New York, 1998).
- Skerry, T.M. & Genever, P.G. Glutamate signalling in non-neuronal tissues. *Trends Pharmacol. Sci.* **22**, 174–181 (2001).
- Hermans, E. & Challiss, R.A. Structural, signalling and regulatory properties of the group I metabotropic glutamate receptors: prototypic family C G-protein-coupled receptors. *Biochem. J.* **359**, 465–484 (2001).
- Aiba, A. et al. Deficient cerebellar long-term depression and impaired motor learning in mGluR1 mutant mice. *Cell* **79**, 377–388 (1994).
- Aiba, A. et al. Reduced hippocampal long-term potentiation and context-specific deficit in associative learning in mGluR1 mutant mice. *Cell* **79**, 365–375 (1994).
- Conquet, F. et al. Motor deficit and impairment of synaptic plasticity in mice lacking mGluR1. *Nature* **372**, 237–243 (1994).
- Dhanasekaran, N., Heasley, L.E. & Johnson, G.L. G protein-coupled receptor systems involved in cell growth and oncogenesis. *Endocr. Rev.* **16**, 259–270 (1995).
- Gutkind, J.S. Cell growth control by G protein-coupled receptors: from signal transduction to signal integration. *Oncogene* **17**, 1331–1342 (1998).
- Takano, T. et al. Glutamate release promotes growth of malignant gliomas. *Nat. Med.* **7**, 1010–1015 (2001).
- Rzeski, W., Turski, L. & Ikonomidou, C. Glutamate antagonists limit tumor growth. *Proc. Natl. Acad. Sci. USA* **98**, 6372–6377 (2001).
- Fрати, C. et al. Expression of functional mGlu5 metabotropic glutamate receptors in human melanocytes. *J. Cell. Physiol.* **183**, 364–372 (2000).
- Jhappan, C. et al. TGF α overexpression in transgenic mice induces liver neoplasia and abnormal development of the mammary gland and pancreas. *Cell* **61**, 1137–1146 (1990).
- Zhu, H., Ryan, K. & Chen, S. Cloning of novel splice variants of mouse mGluR1. *Brain Res. Mol. Brain Res.* **73**, 93–103 (1999).
- Sood, R. et al. Cloning and characterization of a novel gene *SHPRH* encoding a conserved putative protein with SNF2/helicase and PHD-finger domains from 6q24 region. *Genomics* (in the press).
- Zhu, H. et al. Development of early melanocytic lesions in transgenic mice predisposed to melanoma. *Pigment Cell Res.* **13**, 158–164 (2000).